1. Gaussian optics of magnetic lenses

The path of a moving electron in electromagnetic fields ($\vec{E}$ and $\vec{B}$) is governed by the Lorentz equation:

$$m\ddot{\vec{r}} = -e(\vec{E} + \dot{\vec{r}} \times \vec{B}) . \tag{1}$$

Here, a dot indicates a total differentiation with respect to time *t*. Because we restrict our investigations to magnetic fields, the electric field strength $\vec{E}$ is zero. In this case, the absolute value of the velocity is a constant:

$$\left|\dot{\vec{r}}\right| = v = \frac{ds}{dt} = \sqrt{\dot{x}^2 + \dot{y}^2 + \dot{z}^2} = \dot{z}\sqrt{1 + x'^2 + y'^2} = v_0 . \tag{2}$$

Conventional electron microscopes employ exclusively magnetic lenses because their optical performance is superior to that of electrostatic lenses. Therefore, we shall restrict our discussions specific to magnetic elements. By putting $\vec{E} = 0$ in equation (1), we obtain for the motion of the electron in the x and y plane of the Cartesian coordinate the coupled differential equations:

$$\begin{aligned} m\ddot{x} &= e(\dot{z}B_y - \dot{y}B_z), \\ m\ddot{y} &= e(\dot{x}B_z - \dot{z}B_x). \end{aligned} \tag{3}$$

1.1 Conservation of energy

The total energy of the electron, E_{tot} , is conserved in stationary magnetic fields. We choose the gauge of the electric potential Φ in such a way that it vanishes on the cathode surface where the velocity of the electrons is zero, giving

$$E_{\text{tot}} = E_{\text{kin}} + E_{\text{pot}} = 0, \quad E_{\text{kin}} = \frac{m}{2}v^2, \quad E_{\text{pot}} = -e\Phi . \tag{4}$$

From these relations we obtain the electron velocity as

$$v_o = \sqrt{\frac{2e\Phi}{m}} . \tag{5}$$

1.2 Complex notation

The electron trajectory is defined by the two-dimensional vector with the x and y components as function of z in the Cartesian coordinate. Two-dimensional vectors are handled most effectively by employing complex notation. In this notation, the real part of the complex quantity defines the *x*-component and the imaginary part the *y*-component of

the two-dimensional vector. Using the complex notation, the vector of a point from the z axis is $w = x + iy$ and

$$x = \frac{w + \overline{w}}{2}, \qquad y = \frac{w - \overline{w}}{2i}. \tag{6}$$

With $\overline{w} = x - iy.$ is the complex conjugate of w and denoted by a bar. Using the relations (6), we obtain

$$\frac{\partial}{\partial x} = \frac{\partial}{\partial w} + \frac{\partial}{\partial \overline{w}}, \qquad \frac{\partial}{\partial x} + i\frac{\partial}{\partial y} = 2\frac{\partial}{\partial \overline{w}},$$
$$i\frac{\partial}{\partial y} = \left(\frac{\partial}{\partial \overline{w}} - \frac{\partial}{\partial w}\right), \quad \frac{\partial^2}{\partial x^2} + \frac{\partial^2}{\partial x^2} = \left(\frac{\partial}{\partial x} + i\frac{\partial}{\partial y}\right)\left(\frac{\partial}{\partial x} - i\frac{\partial}{\partial y}\right) = 4\frac{\partial^2}{\partial \overline{w}\partial w}. \tag{7}$$

1.3 Power series expansion of the scalar magnetic potential

The stationary magnetic field $\vec{B}$ inside magnetic lens or multipoles or sectors can be described based on the scalar magnetic potential $\psi = \psi(x, y, z)$, which is a useful tool in regions where there is no electric current. The surfaces of magnetic pole pieces form surfaces of constant scalar magnetic potential, $\psi = \psi_o(x, y, z)$. In analogy to the electrostatic case, the magnetic field is given by the gradient of the potential by considering that $\vec{\nabla} \times \vec{B} = 0$:

$$\vec{B} = -\vec{\nabla}\psi. \tag{8}$$

We readily find that the scalar magnetic potential satisfies the Laplace equation

$$\Delta\psi = \vec{\nabla} \bullet \vec{\nabla}\psi = -\vec{\nabla} \bullet \vec{B} = 0. \tag{9}$$

By employing the complex notation as defined in (6), the Laplace equation (9) can be expressed in the form of

$$\Delta\psi = \frac{\partial^2\psi}{\partial x^2} + \frac{\partial^2\psi}{\partial y^2} + \frac{\partial^2\psi}{\partial z^2} = 4\frac{\partial^2\psi}{\partial w \partial \overline{w}} + \frac{\partial^2\psi}{\partial z^2} = 0. \tag{10}$$

In the case of cylindrical symmetry, the magnetic potential depends only on the distance to the cylindrical axis, $\rho^2 = x^2 + y^2 = w\overline{w}$ and the position along the axis, z such as $\psi = \psi(w\overline{w}, z)$. Therefore, the power series expansion of the of the scalar magnetic potential must have the form

$$\psi = \mathrm{Re}\left\{ \sum_{\lambda=0}^{\infty} a_\lambda(z)(w\overline{w})^\lambda \right\}.$$

(11)

Where, Re{} denotes the real part of a complex function. In the case of cylindrical symmetry, it can be shown that the potential is determined entirely by its axial distribution

$$a_0 = a_0(z) = \psi(0,z)\,. \tag{12}$$

Hence, all other coefficients a_λ, for $\lambda > 0$ in (12) must be related in some way with a_0. By substituting the power series expansion (11) for ψ in the Laplace equation (10), we obtain

$$4\sum_{\lambda=1}^{\infty} a_\lambda \lambda^2 (w\overline{w})^{\lambda-1} + \sum_{\lambda=0}^{\infty} a''_\lambda (w\overline{w})^\lambda = 0\,. \tag{13}$$

Here, the prime ' denotes the partial differentiation against the z-coordinate z. In (13), if we replace in the first sum the summation index λ by $\lambda+1$ and consider that the factor of each resulting monomial must vanish owing to the linear independence of different powers of $w\overline{w}$, we readily derive the recurrence formulae

$$4a_{\lambda+1}(\lambda+1)^2 = -a''_\lambda\,, \quad \lambda = 0,1,2,...,\,.$$

(14)

The z-axis forms the optic axis defined by the symmetry axis of the system in case of a cylindrical magnetic lens or by the central trajectory of the electron beam in complex magnetic electron optical systems. Using (14), we obtain the coefficients $a_\lambda(z)$ by means of successive iteration and by assuming that the axial potential $\Psi(z) = a_0$ is known. Starting with $\lambda = 0$ in (14), we readily obtain

$$\begin{aligned}
a_1 &= -\frac{1}{4}a''_0 = -\frac{1}{4}\Psi'', \\
a_2 &= -\frac{1}{4}\frac{1}{4}a''_1 = \frac{1}{4^2}\frac{1}{(2!)^2}\Psi^{[4]}, \\
&\vdots \\
a_\lambda &= (-)^\lambda \frac{1}{4^\lambda}\frac{1}{(\lambda!)}\Psi^{[2\lambda]}.
\end{aligned} \tag{15}$$

By substituting the last expression for a_λ in (11), we obtain for the scalar magnetic potential the power series expansion

$$\psi = \sum_{\lambda=0}^{\infty} (-)^{\lambda} \frac{1}{(\lambda!)^2} \left(\frac{w\overline{w}}{4} \right)^{\lambda} \Psi^{[2\lambda]}(z) \ . \tag{16}$$

The negative derivative of the axial potential $\Psi(z)$ represents the magnetic field strength along the optic axis

$$B_z(0,z) = B(z) = -\Psi'(z) \ . \tag{17}$$

By using this relation and the expression (16), we eventually obtain by differentiation the components of the rotationally symmetric magnetic field as

$$\begin{aligned} B_z(w,\overline{w},z) &= -\frac{\partial \psi}{\partial z} = \sum_{\lambda=0}^{\infty} (-)^{\lambda} \frac{1}{(\lambda!)^2} \left(\frac{w\overline{w}}{4} \right)^{\lambda} B^{[2\lambda]}(z), \\ B_x + iB_y &= -2\frac{\partial \psi}{\partial \overline{w}} = \frac{w}{2} \sum_{\lambda=0}^{\infty} (-)^{\lambda+1} \frac{1}{\lambda!(\lambda+1)!} \left(\frac{w\overline{w}}{4} \right)^{\lambda} B^{[2\lambda+1]}(z). \end{aligned} \tag{18}$$

1.4 Paraxial approximation

The electron beam angle is small in a magnetic lens (on the order of ~10 mrads) and the electron trajectory is confined mostly to the vicinity of the optical axis. The paraxial approximation ignores the small curvatureof the electron trajectory. This approximation has a sufficient degree of accuracy for describing the propagation of electrons confined to the vicinity of the optic axis.

We choose the optic axis as the *z*-axis of the Cartesian *x,y,z* -coordinate system. The components of the velocity of the electron are related with the slope components x', y' of its trajectory by

$$\begin{aligned} \frac{v_x}{v} &= \frac{dx/dt}{ds/dt} = \frac{dx}{ds} = \frac{x'}{\sqrt{1+x'^2+y'^2}}, \\ \frac{v_y}{v} &= \frac{dy/dt}{ds/dt} = \frac{dy}{ds} = \frac{y'}{\sqrt{1+x'^2+y'^2}}, \\ \frac{v_z}{v} &= \frac{dz/dt}{ds/dt} = \frac{dz}{ds} = \frac{1}{\sqrt{1+x'^2+y'^2}}. \end{aligned} \tag{19}$$

Paraxial approximation neglects the quadratic terms x'^2 and y'^2 in the expressions (19), giving

$$\dot{x} = v_x \approx vx', \quad \dot{y} = v_y \approx vy', \quad \dot{z} = v_z \approx v\,. \tag{20}$$

These are the paraxial path equations, which are linear between the off-axial position and the slope of the trajectory. Because of this, it suffices to consider only the axial field component $B = B(z) = B_z(z, x = 0, y = 0)$ and the linear terms of the lateral components of the magnetic field, which are given by the first term of the second power series in (18):

$$B_x + iB_y = -\frac{B'}{2}(x + iy)\,. \tag{21}$$

In order to simplify the paraxial path equation, we introduce the rotating u, z -coordinate system. Within the frame of this system the lateral position of the electron is given by $u(z) = u_r(z) + iu_i(z)$, as depicted in Fig. 1.

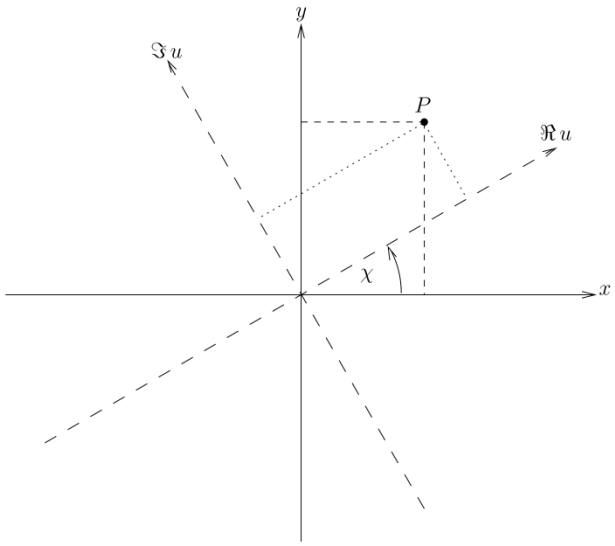

Fig. 1: Position *P* of the electron in the fixed *x, y* coordinate system and in the rotating u_r, u_i coordinate system ($u_r = \mathrm{Re}\,u, u_i = \mathrm{Im}\,u$), respectively; $2\chi = 2\chi(z)$ is the Larmor angle.

The lateral position coordinates of the electron in the fixed coordinate system of x,y are related with those in the rotating coordinate by

$$w(z) = x(z) + iy(z) = u(z)e^{i\chi(z)} \tag{22}$$

By employing the approximations (20) and (21), we derive from (2) the paraxial equations of motion as

$$
\begin{aligned}
m\ddot{x} &\approx mv^2 x'' = e(\dot{z}B_y - \dot{y}B_z) \approx -ev(y'B + yB'/2), \\
m\ddot{y} &\approx mv^2 y'' = e(\dot{x}B_z - \dot{z}B_x) \approx ev(x'B + xB'/2).
\end{aligned}
\tag{23}
$$

We multiply the second equation by the imaginary unit i and add the resulting equation to the first equation in (23), giving the complex equation

$$
w'' - i\frac{eB}{mv}w' - i\frac{eB'}{2mv}w = 0 . \tag{24}
$$

In order to obtain an equation with real coefficients, we transform this equation by means of (22). Differentiating this relation twice, gives

$$
\begin{aligned}
w &= ue^{i\chi} \\
w' &= (u' + iu\chi')e^{i\chi}, \\
w'' &= (u'' + 2i\chi'u' + i\chi''u - \chi'^2 u)e^{i\chi}.
\end{aligned}
\tag{25}
$$

Substituting w, w', w'' in (24) by the expressions (25), we obtain the rather involved transformed equation

$$
u'' + 2i\chi'u' + i\chi''u - \chi'^2 u - i\frac{eB}{mv}(u' + i\chi'u) - i\frac{eB'}{2mv}u = 0 .
\tag{26}
$$

We simplify considerably this rather involved equation by choosing

$$
\chi' = \frac{eB}{2mv} = \sqrt{\frac{e}{8m\Phi}}B \ . \tag{27}
$$

In this case, several terms cancel out and equation (26) adopts the simple form

$$
u'' + \frac{eB^2}{8m\Phi}u = 0 . \tag{28}
$$

The integration of (27) gives the rotation angle

$$
\chi = \sqrt{\frac{e}{8m\Phi}}\int_{z_o}^{z} B dz . \tag{29}
$$

This angle vanishes at the object plane $z = z_o$, or $\chi(z = z_o) = 0$ where the rotating coordinate system coincides with the fixed coordinate system.

The paraxial path equation (28) is a linear second-order differential equation which has two linearly independent solutions. Proper solutions are the so-called fundamental rays u_α and u_γ which are real functions of z. Any other solution is a linear combination of these two basic solutions.

The axial fundamental ray u_α starts from the center of the object plane with unit slope. Hence it satisfies the initial conditions

$$u_\alpha(z_o) = 0, \qquad u'_\alpha(z_o) = 1. \tag{30}$$

The field ray u_γ starts at position $u_o = 1$ at the object plane and intersects the center of the aperture plane $z = z_a$. Hence this ray satisfies the boundary conditions

$$u_\gamma(z_o) = 1, \qquad u_\gamma(z_a) = 0. \tag{31}$$

This ray is chosen if the trajectory is fixed by its points of intersection u_o and u_a with object plane and the aperture plane, respectively. If the ray is fixed by its position $u_o = w_o = x_o + iy_o$ and its slope $u'_o = \alpha + i\beta$ at the object plane z_o, then it is more appropriate to use the principal ray u_π instead of u_γ. The principal ray satisfies the boundary conditions

$$u_\pi(z_o) = 1, \qquad u'_\pi(z_o) = 0. \tag{32}$$

Similarly, any other ray can be written as a linear combination of the axial ray and the principle ray. It should be noted that although the fundamental rays are real, a general solution will be complex. To demonstrate this behavior, we consider a ray which starts at the object plane from the point u_o with slope u'_o. The course of this ray is given by the linear combination

$$u = u_o u_\pi + u'_o u_\alpha. \tag{33}$$

This expression represents a complex solution of the path equation (28) because the coefficients u_o and u'_o are complex quantities characterized by their amplitudes and angles. It must be emphasized that in order that this ray propagates within the paraxial approximation regime, the initial slope must be very small ($|u'_o| << 1$).

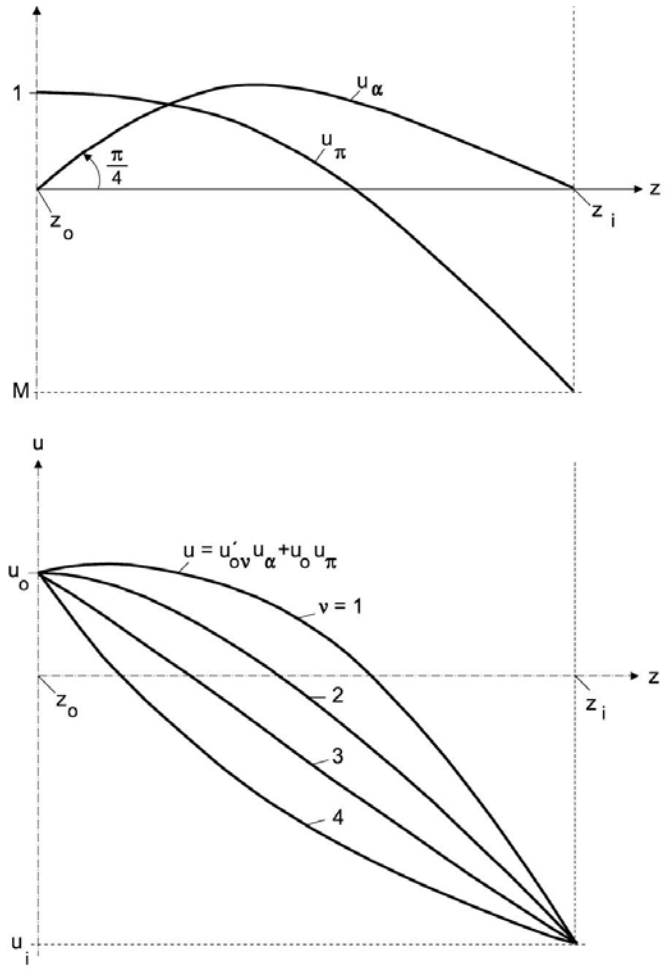

Fig. 2: Trajectories of the axial fundamental ray u_α and of the principal ray u_π between the object plane z_o and the image plane z_i (upper diagram), and courses of the trajectories of a pencil of rays from a point on the object plane illustrating the formation of the image (lower diagram)

The general solution (32) of the path equation (28) describes entirely the imaging properties of magnetic lenses in paraxial approximation. The zeros of the axial fundamental ray u_α determine the locations of the images, as shown in Fig. 2 for a single image. Several images are formed in an electron microscope. Owing to the linearity of the paraxial approximation, all rays emanating from any object point u_o intersect the image point $u_i = u(z_i) = u_o u_\pi(z_i) + u_o' u_\alpha(z_i) = u_o u_\pi(z_i)$. The image plane $z = z_i$ is a conjugate of the object plane. The value of the field ray and/or that of the principal ray at the image plane determine the magnification

$$M = \frac{u_i}{u_o} = u_\gamma(z_i) = u_\pi(z_i)\,. \tag{34}$$

The last relation holds true because u_π must be a linear combination of u_γ and of u_α

1.5 Helmholtz-Lagrange relation

The Helmholtz-Lagrange (HL) relation connects the lateral positions and slopes of any two trajectories with each other. As a result, the courses of the trajectories of a bundle of rays are ordered in some way. For example, the trajectories of a concentric bundle of rays are perpendicular to the surfaces of constant phase of the associated spherical wave which emanates from the common center of the trajectories, as illustrated in Fig. 3.

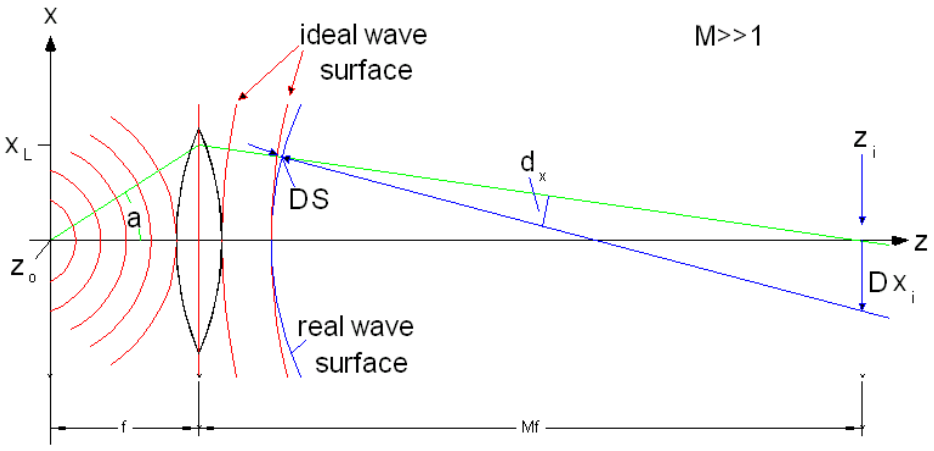

Fig. 3: Illustration of the particle and wave property of electrons. The rays emanating from the center of the object plane are orthogonal to the surfaces of constant phase of the associated elementary wave. The electron lens transforms the spherical incident wave in a converging non-spherical outgoing wave. The deviation *Ds* of the wave surface from its ideal spherical shape induces the aberration Dx_i at the image plane.

Considering the two linearly independent fundamental rays u_α and u_γ, each of which satisfies the path equation (28). We multiply the equation for u_α by u_γ and that for u_γ by $-u_\alpha$, giving

$$\begin{aligned} u_\gamma\left(u_\alpha'' + \chi'^2 u_\alpha = 0\right), \\ -u_\alpha\left(u_\gamma'' + \chi'^2 u_\gamma = 0\right) \end{aligned} \tag{35}$$

By adding these equations, we obtain

$$u_\gamma u_\alpha'' - u_\alpha u_\gamma'' = \frac{d}{dz}\left(u_\gamma u_\alpha' - u_\alpha u_\gamma'\right) = 0\,. \tag{36}$$

The integration of the total differential readily gives the relation

$$u_\gamma u'_\alpha - u_\alpha u'_\gamma = \text{const} = 1. \tag{37}$$

This is known as the HL relation, which is given by the Wronski determinant in Gaussian approximation.

If we apply this relation to the image plane $z = z_i$, we obtain

$$M = \frac{u(z_i)}{u(z_o)} = u_\gamma(z_i) = \frac{1}{u'_\alpha(z_i)} = \frac{u'(z_o)}{u'(z_i)}. \tag{38}$$

This formula coincides with that of light optics which states that the magnification in paraxial approximation is determined entirely by the ratio of the object slope and the image of any axial ray.

1.6 Theorem of alternating images

Another important consequence of the HL relation is the *theorem of alternating images.* Within a multi-stage imaging system, such as an electron microscope, a plane will be imaged repeatedly throughout the imaging system. As an example, we consider the formation of the images of two apertures *A* and *C* placed at planes $z = z_\alpha$ and $z = z_\gamma$, as depicted in Fig. 4. Typical plane locations are the object plane and the back focal plane of a lens in a imaging system. The back focal plane is an image plane of the source for parallel illumination. Without loss of generality, we center one aperture at the object plane $z_\alpha = z_o$ and the other at an image $z_\gamma = z_s$ of the *effective* source. As the pair of linearly independent trajectories, we select the fundamental rays u_α and u_γ.

The ray u_α intersects the center of the aperture *A*, the ray u_γ that of the aperture *C*:

$$u_\alpha(z_\alpha) = 0 \ , \quad u_\gamma(z_\gamma) = 0 . \tag{39}$$

Consecutive images of the apertures *A* and *C* are formed at the planes $z_{\alpha n}$ and at the planes $z_{\gamma n}$, $n = 1,2,...$, respectively. By taking the Wronskian (HR relation) of the two rays at any two subsequent images A_n and A_{n+1} of the aperture *A*, we obtain the relation

$$\left(u_\gamma u'_\alpha\right)_{z_{\alpha n}} = \left(u_\gamma u'_\alpha\right)_{z_{\alpha,n+1}} . \tag{40}$$

Since $u_\alpha(z_{\alpha n}) = u_\alpha(z_{\alpha,n+1}) = 0$, the slopes of u_α at the planes $z_{\alpha n}$ and $z_{\alpha,n+1}$ must have *opposite* sign, as demonstrated in Fig. 4. Considering this behavior, it readily follows from (40) that u_γ must change its sign in the region between two subsequent images of the aperture *A*. This is only possible if an image ($u_\gamma(z_{\gamma n}) = 0$) of the aperture *C* is located in this domain.

Accordingly, we can state: "*An optical system always forms an image of the source in the domain between any two subsequent images of the object plane*".

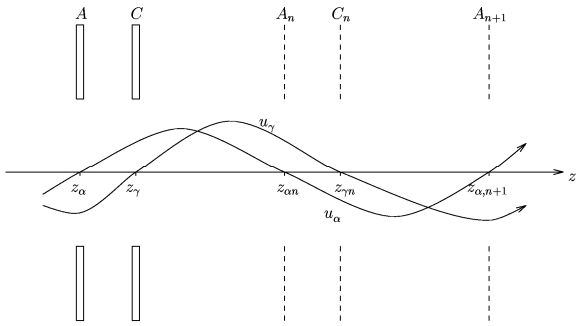

Fig. 4: Illustration of the theorem of alternating images

Figure 4 illustrates the consequences of this theorem for the image formation in an ideal electron microscope. The crossover of the cathode defines the effective source, which is located at some distance from the surface of the emitter. For a field emission gun, the crossover is generally virtual and located inside the tip of the emitter. The condenser system adjusts the illumination of the object. In order to achieve an ideal illumination system, the condenser should consist of two lenses and two apertures, one placed at the image of the crossover, the other (illumination aperture) at an image of the cathode surface. The condenser lenses image the crossover aperture onto the object plane. This aperture limits the field of illumination, whereas the illumination aperture determines the maximum angle of illumination.

A very suitable kind of illumination is the "*Koehler illumination*", which is largely employed in light microscopy and illustrated in Fig. 5. This illumination is realized by adjusting the condenser lenses in such a way that an image of the surface of the cathode is formed at the back focal plane of the objective lens. The Koehler illumination has the advantage that local variations of the electron emission on the cathode surface do not show up as artifacts in the image of the object. We can vary the location of the crossover image by changing the illumination mode. For Koehler illumination, the back focal plane of the objective lens is also the diffraction plane of the object. In accordance with the famous optician E.Abbe, one defines the diffraction pattern at this plane as the "*primary image*".

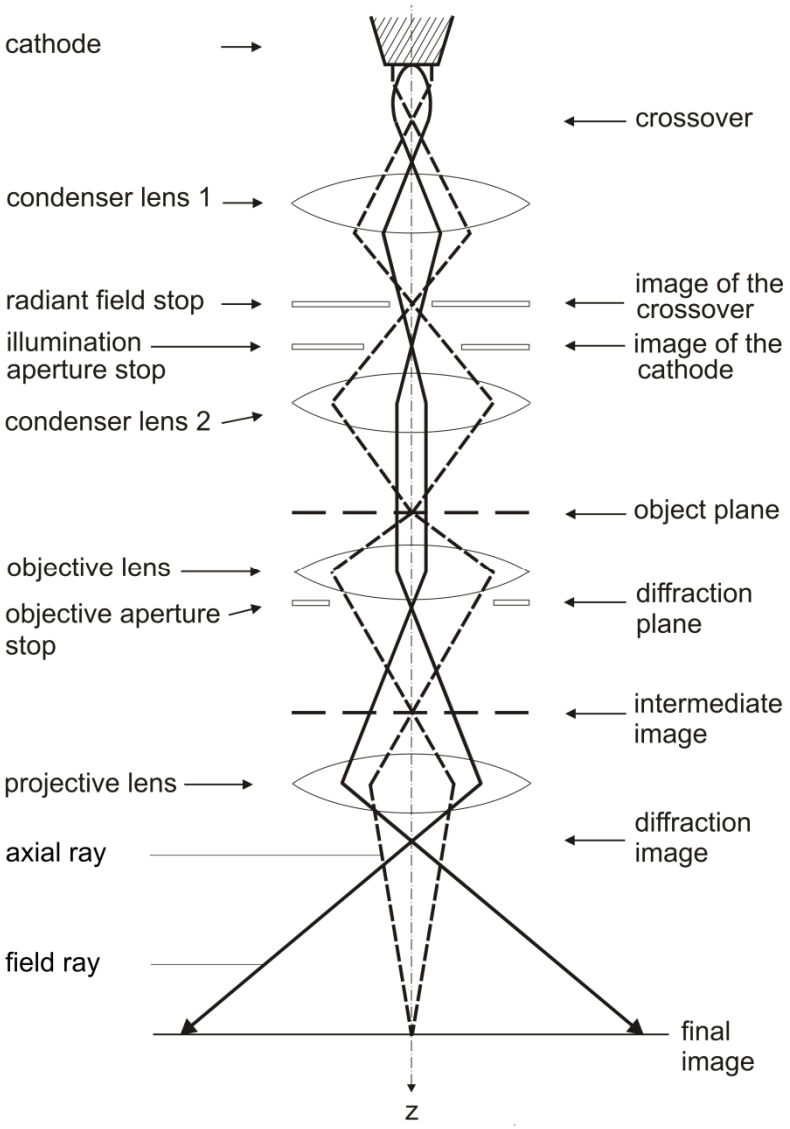

Fig. 5: Scheme of the path of the fundamental paraxial trajectories and location of the images and beam-limiting apertures in a transmission electron microscope illustrating the theorem of alternating images

1.7 Cardinal elements of thin magnetic lenses

We define a lens as thin if the axial extension of its magnetic field is significantly smaller than its focal length *f*. This condition is fulfilled if the principal ray changes its direction but not appreciably its lateral distance within the field of the lens ($u_\pi \approx 1$). Moreover, we impose that the object plane is located in field-free space in front of the lens. The cardinal elements of the lens are determined by the asymptotes of the principal ray u_π which satisfies the initial conditions

$$u_\pi(-\infty) = 1, \quad u'_\pi(-\infty) = 0. \tag{41}$$

Accordingly, the incident asymptote of this trajectory is parallel to the optic axis. We obtain its image asymptote by transforming the differential equation (28) into an integral equation. For reasons of mathematical simplicity we write

$$T = T(z) = \chi'^2 = \frac{eB^2}{8\Phi m}. \tag{42}$$

By considering the boundary conditions (41) and by performing partial integrations of equation (28), we eventually arrive at the integral equation (hint: use the relationship of $xf\left(x\right) = \int f(x)dx + \int xf(x)dx$)

$$\begin{aligned} u_\pi &= 1 - \int_{-\infty}^{z}\int_{-\infty}^{\zeta} T(\xi)u_\pi(\xi)d\xi d\zeta = \\ &1 - z\int_{-\infty}^{z} T(\zeta)u_\pi(\zeta)d\zeta + \int_{-\infty}^{z} \zeta T(\zeta)u_\pi(\zeta)d\zeta. \end{aligned} \tag{43}$$

The above equation incorporated the boundary conditions in (41), the solution of the integral equation is thus unique. Within the conditions for the thin lens approximation, the principal ray changes its direction but not appreciably its initial off-axial distance $u_\pi(-\infty) = 1$ within the field of the thin lens so that

$$Tu_\pi \approx T. \tag{44}$$

By employing this approximation, we obtain from (43) the emergent asymptote of the principal ray as

$$\begin{aligned} u_{\pi,as} &= 1 - (z - z_l)\int_{-\infty}^{\infty} T(z)dz. \\ z_l &= \frac{\int_{-\infty}^{\infty} zT(z)dz}{\int_{-\infty}^{\infty} T(z)dz}. \end{aligned} \tag{45}$$

Here z_l defines the location of the center of gravity of the strength T of the magnetic lens. The upper limit of the integration is taken to infinite since beyond the lens field, $T(z) = 0$. The emergent asymptote (45) intersects the optic axis at the image focal plane

$$z_F = z_l + \frac{1}{\int_{-\infty}^{\infty} T(z)dz}. \tag{46}$$

The incident and emergent asymptotes of the principal ray define the cardinal points of the lens, as depicted in Fig. 6. The asymptotes of this trajectory intersect each other at the image principal plane z_P which coincides with the central plane z_l of the magnetic lens.

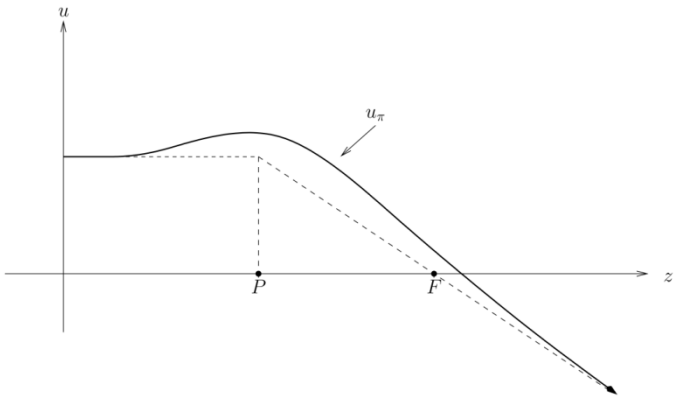

Fig. 6: Definition of the image focal point *F* and the image principal point *P* by means of the asymptotes of the principal ray u_π

At $z_P = z_l$, the two asymptotes intersect, which defines the principal plane. The focal length *f* of the thin magnetic lens is given by the distance $z_F - z_P = z_F - z_l$ between the focal plane and the principal plane By considering this relation, we readily obtain Busch's formula for the reciprocal focal length of a short magnetic lens

$$\frac{1}{f} = \int_{-\infty}^{\infty} T dz = \int_{-\infty}^{\infty} \frac{eB^2}{8m\Phi} dz \,. \tag{47}$$

Since the focusing strength *T* is positive definite, it follows that all short magnetic electron lenses are convergent.

The asymptotes of the object principal ray $u_{\bar{\pi}}$ from ∞ determine the object cardinal points $\bar{P}$ and $\bar{F}$ of the lens (the front principal and focal planes). We readily obtain this ray by following the same method used for the principal ray about the plane $z_P = z_l$. As a result, the object principal plane $z_{\bar{P}}$ coincides with the image principle plane z_P, and the object focal point $\bar{F}$ has the same distance from the central plane $z_l = z_P = z_{\bar{P}}$ as the image focal point *F*. We use the principal rays to illustrate the Gaussian image construction by means of the cardinal elements. For this purpose, we express the fundamental axial ray as linear combination $u_\alpha = C_1 u_\pi + C_2 u_{\bar{\pi}}$ of the two principal rays. We determine the coefficients by imposing on the linear combination the initial conditions (30) for the axial ray, giving

$$u_\alpha = \frac{1}{u'_{\bar{\pi}}(z_o)} \left(u_{\bar{\pi}} - u_{\bar{\pi}}(z_o) u_\pi \right) = f u_{\bar{\pi}} + (z_{\bar{F}} - z_0) u_\pi \,. \tag{48}$$

Because the image is formed in field-free space on the far side of the lens, the course of the axial ray in this region is determined by the image asymptotes of the principal rays. Substituting these asymptotes for $u_{\bar{\pi}}$ and u_{π} in (48), obtain

$$u_{\alpha} = f - (z_{\bar{F}} - z_0)\frac{z - z_F}{f} \quad . \tag{49}$$

By considering that $u_{\alpha} = 0$ at the image plane $z = z_i$, we readily derive Newton's formula of light optics

$$(z_{\bar{F}} - z_0)(z_i - z_F) = f^2 . \tag{50}$$

The Gaussian construction of the image by means of the cardinal points is the equivalent geometrical result, as depicted in Fig. 6.

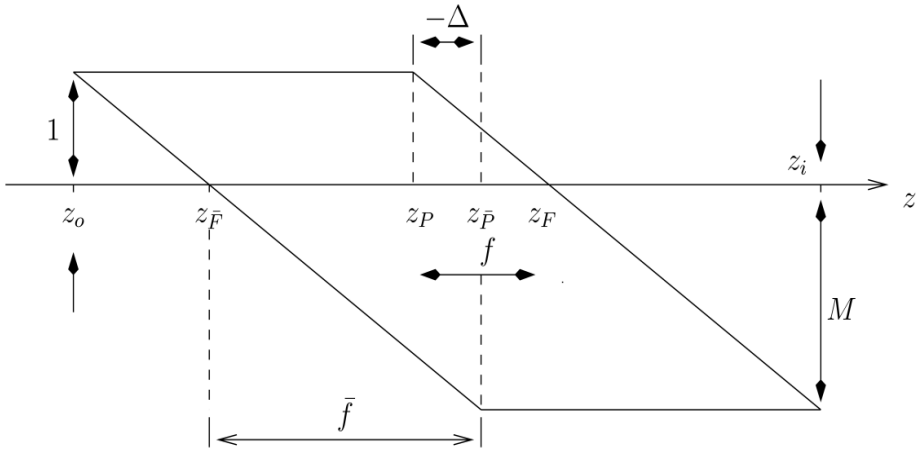

Fig. 6: Gaussian image construction by means of the cardinal points. In the case of thin magnetic lenses, the object and image principle planes $z_P, z_{\bar{P}}$ and the focal lengths $f, \bar{f}$ coincide ($\Delta = z_P - z_{\bar{P}} = 0$, $f = \bar{f}$).

2. Multipoles

Multipoles are elements which are formed by separate identical poles or electrodes placed symmetrically about the optic axis. Magnetic multipole fields are formed by currents within the coils around each pole piece. The absolute value of the currents is the same but their directions are opposite for any two neighboring coils. Electrostatic multipole fields are formed by applying a voltage with alternating sign to the electrode. The formations of a magnetic quadrupole field and of an electrostatic quadrupole field are illustrated in Figs. 7a and 7b. A multipole field of multiplicity *m* is formed by 2*m* poles or

electrodes, respectively. To survey the electron optical properties of multipole fields, we first consider plane multipole potentials formed within multipoles whose extension along the optic axis is very large compared with the distance of their pole pieces and/or electrodes from the optic axis. In this case, the interior magnetic potential $\psi = \psi(x, y)$ and/or the electrostatic potential $\varphi = \varphi(x, y)$ are two-dimensional independent of z.

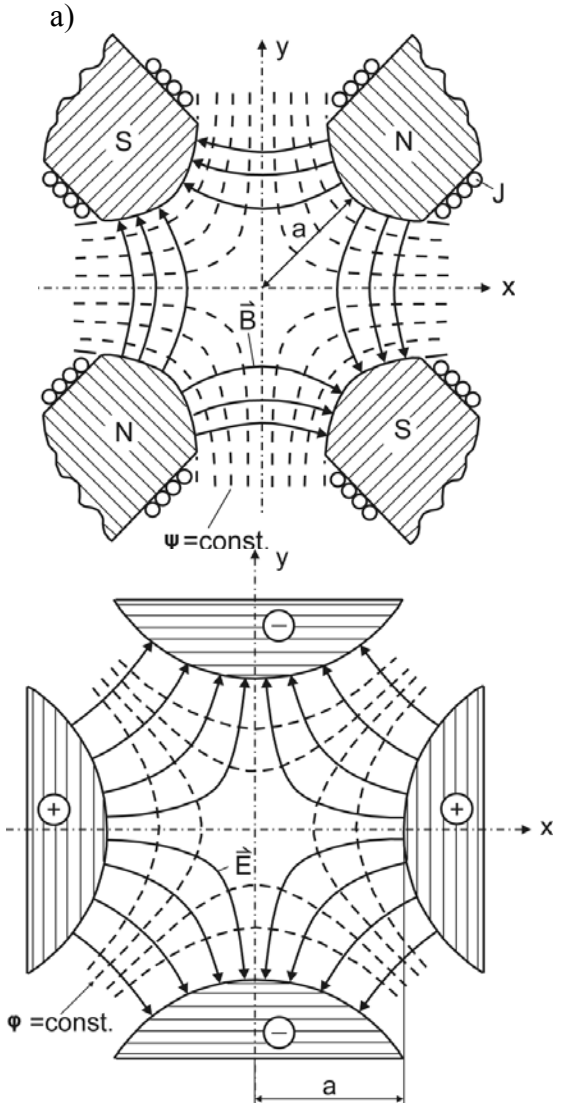

Fig. 7: Cross-section, field lines and lines of constant potential of (a) a magnetic quadrupole and (b) an electrostatic quadrupole. Both quadrupoles focus the electrons in the *x*,*z*-section and defocus them in the *y*,*z*-section.

Magnetic quadrupoles serve as so-called *stigmators* (“point maker”) in the electron microscope to compensate for the parasitic axial astigmatism caused by the unavouidable deviations of the electromagnetic fields from ideal cylindrical symmetry.

2.1 Planar multipoles

For reasons of simplicity we consider the planar (two-dimensional) electrostatic potential which satisfies the two-dimensional Laplace equation

$$\Delta\varphi = \frac{\partial^2\varphi}{\partial x^2} + \frac{\partial^2\varphi}{\partial y^2} = 4\frac{\partial^2\varphi}{\partial w \partial \overline{w}} = 0\,. \tag{51}$$

According to the second relation in (51) the general solution has the form

$$\varphi = \mathrm{Re}\, F(\overline{w}) = \frac{1}{2}\left\{F(\overline{w}) + \overline{F}(w)\right\}. \tag{52}$$

Here $F(\overline{w})$ is an arbitrary complex analytical function of the variable $\overline{w} = x - iy = \rho e^{-i\phi}$. The potential of a plane electrostatic multipole with multiplicity *m* is given by the harmonic polynomial

$$\begin{aligned} \varphi = \varphi_m &= \mathrm{Re}(\Phi_m \overline{w}^m) = \rho^m[\Phi_{mc}\cos m\phi + \Phi_{ms}\sin m\phi] \\ &= \left|\Phi_m\right|\rho^m \cos m(\phi - \alpha_m) \end{aligned}\,. \tag{53}$$

The real part and the imaginary part of the complex multipole strength Φ_m depend on the angular orientation α_m of the electrodes with respect to the axes of the coordinate system:

$$\Phi_m = \Phi_{mc} + i\Phi_{ms} = \left|\Phi_m\right| e^{im\alpha_m}\ ,\ \alpha_m = \frac{1}{m}\arctan(\Phi_{ms}/\Phi_{mc})\,. \tag{54}$$

To elucidate the focusing properties of an electrostatic multipole, we choose as an important example the quadrupole whose potential is depicted in Fig. 8.

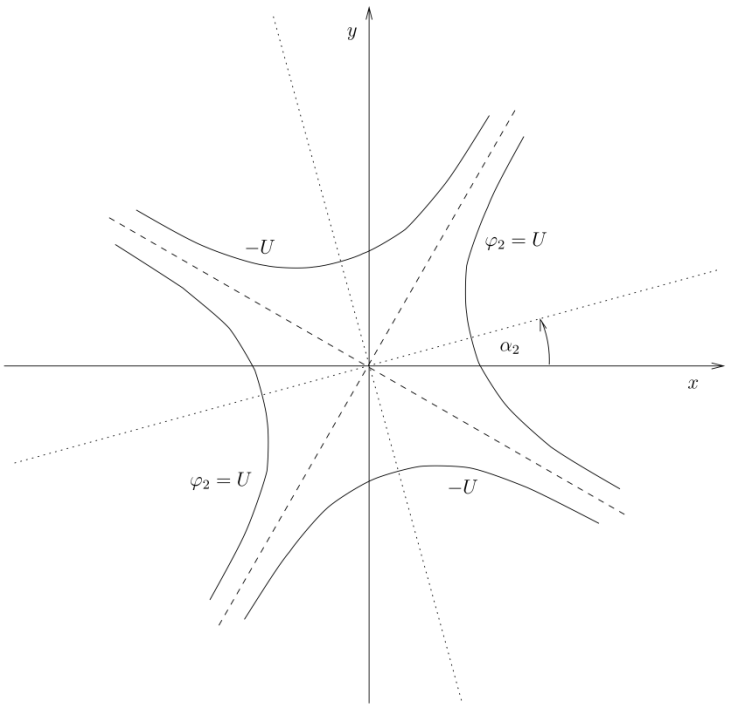

Fig.8: Equipotentials of a plane quadrupole whose principal sections (dotted lines) are rotated by the angle α_2 with respect to the *x*- and *y*-axis, respectively.

The equipotentials form the hyperbolas

$$\begin{aligned} \varphi_2 &= \mathrm{Re}\{\Phi_2 \overline{w}^2\} = |\Phi_2| \rho^2 \cos 2(\phi - \alpha_2) \\ &= \Phi_{2c}(x^2 - y^2) + 2\Phi_{2s} xy = \text{const.} \end{aligned} \tag{55}$$

Differentiation with respect to $\overline{w}$ gives

$$\nabla \varphi_2 = 2 \frac{\partial \varphi_2}{\partial \overline{w}} = -E_x - iE_y == 2\Phi_2 \overline{w} \,. \tag{56}$$

Therefore, the electric force $F_x + iF_y = e2\Phi_2 \overline{w}$ depends linearly on the distance of the electron from the optic axis, as it is the case for round lenses. In the special case $\alpha_2 = \Phi_{2s} = 0$, the electrodes are centered along the coordinate axes, as shown in Fig.7. In this case the components of the electric force are

$$F_x = 2e\Phi_{2c} x \,, \qquad F_y = -2e\Phi_{2c} y \,. \tag{57}$$

These relations show that an electron which propagates in *z*-direction within one of the two symmetry sections *x,z* (*y=0*) or *y,z* (*x=0*) does not experience a perpendicular force and will remain in this section along its entire path. Since the components (57) of the

electric force have opposite signs, the quadrupole *focuses* the charged particles in one principal section and *defocuses* them in the other.
Another important multipole element is the hexapole which is the basic element of correctors compensating for the spherical aberration of the round lenses of electron microscopes. The potential of a planar hexapole is given by

$$\begin{aligned}\varphi_3 &= \mathrm{Re}\{\Phi_3 \overline{w}^3\} = |\Phi_3|\rho^3 \cos 3(\phi - \alpha_3) \\ &= \Phi_{3c}(x^3 - 3xy^2) - \Phi_{3s}(y^3 - 3x^2 y) = \text{const.}\end{aligned} \tag{58}$$

The action of the hexapole force on electrons travelling in z-direction is shown in Fig. 9.

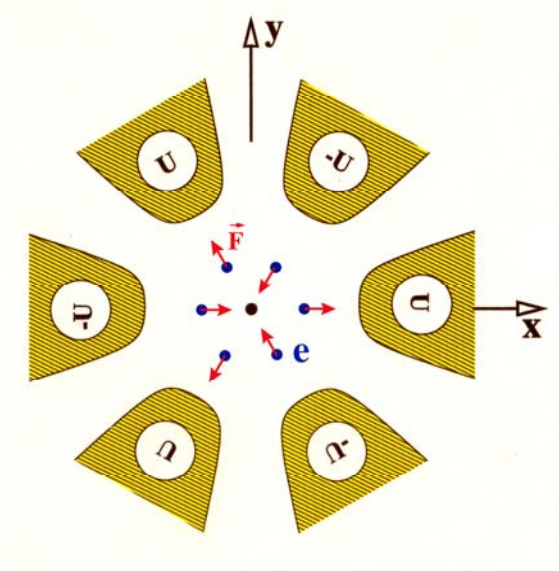

Fig. 9: Arrangement of the electrodes of an electrostatic hexapole element and action of its field on electrons propagating parallel to the optic axis.

We readily obtain the scalar potential $\psi_m, m = 2,3,...,$ of two-dimensional magnetic multipoles from the equivalent electrostatic potentials by substituting ψ_m for φ_m and Ψ_m for Φ_m in the expressions (51-58).

2.2 Three-dimensional multipoles

We have shown that the harmonic polynomials represent multipole solutions of the two-dimensional Laplace equation. These solutions of the potential are realized within infinitely extended multipole elements. In order to find the three-dimensional scalar magnetic potential of multipole fields with finite extension along the optic axis, we must consider the multipole strengths Ψ_m as functions of the *z*-coordinate.

In the region outside of the pole pieces we can decompose the scalar potential ψ of any magnetic system in a sum of multipole terms ψ_m about a common straight axis:

$$\psi = \sum_{m=1}^{\infty} \psi_m \,. \tag{59}$$

This decomposition corresponds to a Fourier series expansion with respect to the azimuth angle ϕ about the optic axis. Owing to these considerations, the power series expansion of the component ψ_m of the scalar magnetic potential must have the form

$$\psi_m = \mathrm{Re}\left\{ \sum_{\lambda=0}^{\infty} a_{m\lambda}(z)(w\overline{w})^{\lambda}\, \overline{w}^{m} \right\}. \tag{60}$$

The coefficients $a_{m\lambda}(z)$ are generally complex. The first coefficient $a_{m0}(z) = \Psi_m(z)$ defines the multipole strength, as in the planar case $(a_{m\lambda} = 0, m > 0)$. The power of order λ describes the dependence of the magnetic potential on distance to the multipole axis using Taylor expansion. We derive the coefficients $a_{m\lambda}(z)$ with $\lambda > 0$ by inserting the expansion (60) in the Laplace equation (10). By employing the same procedure as in the rotationally symmetric case $m = 0$, we eventually obtain the recurrence formula

$$4a_{m,\lambda+1}(\lambda + m + 1)(\lambda + 1) = -a''_{m\lambda}\,, \quad \lambda = 0,1,2,... \quad . \tag{61}$$

By staring with $\lambda = 0$, we derive by successive iteration the relation

$$a_{m\lambda} = (-)^{\lambda} \frac{1}{4^{\lambda}\lambda!} \frac{m!}{(\lambda + m)!} \Psi_m^{[2\lambda]}. \tag{62}$$

By substituting this expression for $a_{m\lambda}$ in (60), we obtain for the scalar potential of a magnetic multipole with multiplicity *m* the power series expansion

$$\psi_m = \sum_{\lambda=0}^{\infty} (-)^{\lambda} \frac{m!}{\lambda!(\lambda + m)!} \left(\frac{w\overline{w}}{4} \right)^{\lambda} \mathrm{Re}\left\{ \Psi_m^{[2\lambda]}(z)\overline{w}^{m} \right\}. \tag{63}$$

By putting $m = 0$ and considering $0! = 1$, we obtain the power series (10) for the scalar magnetic potential of rotationally symmetric systems.

3. Aberrations

Aberrations are caused by the inherent defects of electron lenses. These defects are caused by the non-linear off-axial terms of the magnetic field expansion (18) and by the quadratic terms of the slope components in the exact path equation

$$\frac{d(v_x/v)}{dz}=\frac{d}{dz}\left(\frac{x'}{\sqrt{1+x'^2+y'^2}}\right)=-\frac{e}{mv}\left(\frac{v_y}{v_z}B_z-B_y\right)=-\frac{e}{mv}\left(y'B_z-B_y\right),$$
$$\frac{d(v_y/v)}{dz}=\frac{d}{dz}\left(\frac{y'}{\sqrt{1+x'^2+y'^2}}\right)=\frac{e}{mv}\left(\frac{v_x}{v_z}B_z-B_x\right)=\frac{e}{mv}\left(x'B_z-B_x\right). \tag{64}$$

We combine the two equations to a single equation for the complex lateral distance $w=w(z)=x(z)+iy(z)$ by multiplying the second equation with the imaginary unit and adding the resulting equation to the first equation, giving

$$\frac{d}{dz}\left(\frac{w'}{\sqrt{1+w'\overline{w}'}}\right)=-\frac{ie}{mv}\left(B_x+iB_y-w'B_z\right)=\frac{ie}{mv}\left(2\frac{\partial\psi}{\partial\overline{w}}-w'\frac{\partial\psi}{\partial z}\right). \tag{65}$$

By employing the power series expansions (59) and (63) for the scalar magnetic potential, we obtain for the components of the magnetic field strength the expressions

$$B_z(w,z)=-\frac{\partial\psi}{\partial z}=-\sum_{m=0}^{\infty}\sum_{\lambda=0}^{\infty}(-)^{\lambda}\frac{m!}{\lambda!(\lambda+m)!}\left(\frac{w\overline{w}}{4}\right)^{\lambda}\mathrm{Re}\left\{\Psi_m{}^{[2\lambda+1]}(z)\overline{w}^m\right\}, \tag{66}$$

$$\begin{aligned}B_x+iB_y&=-2\frac{\partial\psi}{\partial\overline{w}}\\&=-\sum_{m=0}^{\infty}\sum_{\lambda=0}^{\infty}(-)^{\lambda}\frac{m!}{\lambda!(\lambda+m)!}\left(\frac{w\overline{w}}{4}\right)^{\lambda}\left\{(\lambda+m)\overline{w}^{m-1}\Psi_m^{[2\lambda]}+\lambda w^{m-1}\overline{\Psi}_m^{[2\lambda]}\right\}.\end{aligned} \tag{67}$$

3.1 Power series representation of the path equation

We aim to establish a convenient procedure which yields consecutively the aberrations with increasing order. The aberrations of order *n* are polynomials of order *n* in the ray parameters $\omega,\overline{\omega},w_o,\overline{w}_o$. The higher the order of an aberration is, the less affects the aberration the image quality because the angles $|\omega|$ and $|w_o/f|$ are very small ($|\omega_{\max}|<<1$, $|w_o/f|_{\max}<<1$) in an electron microscope. Owing to this behavior it, is advantageous to look for a procedure giving the aberrations by successive iteration in increasing order. We obtain an appropriate method by writing the path equation (65) as a power series in the off-axial quantities $w,\overline{w},w'$ and $\overline{w}'$.

To reduce the size of the mathematical expressions, we confine our considerations to the important cases of magnetic round lenses and hexapole correctors. In this case, we must take into account only the terms with multiplicity $m=0$ and $m=3$ in the expressions (66) and (67) for the components of the magnetic field strength. By substituting the

resulting expressions for the components of the magnetic field for those in equation (65), we eventually obtain

$$\frac{d}{dz}\left(\frac{w'}{\sqrt{1+w'\overline{w}'}}\right)=\frac{2w''+w'(w''\overline{w}'-\overline{w}''w')}{2\left(1+w'\overline{w}'\right)^{3/2}}=i\frac{e}{mv}\left(2\frac{\partial\psi}{\partial\overline{w}}-w'\frac{\partial\psi}{\partial z}\right) \tag{68}$$

To eliminate the nonlinear term $w'(w''\overline{w}'-\overline{w}''w')$, we multiply (68) by $\overline{w}'$, the conjugate complex equation by w' and subtract the resulting equations from each other, giving

$$\frac{(w''\overline{w}'-\overline{w}''w')}{\left(1+w'\overline{w}'\right)^{1/2}}=i\frac{2e}{mv}\left(\overline{w}'\frac{\partial\psi}{\partial\overline{w}}+w'\frac{\partial\psi}{\partial w}-w'\overline{w}'\frac{\partial\psi}{\partial z}\right). \tag{69}$$

By inserting this expression into (68), we eventually obtain after a straightforward calculation the path equation in the appropriate form

$$\begin{aligned}
w''&=\frac{ie}{mv}\left(1+w'\overline{w}'\right)^{1/2}\left(2\frac{\partial\psi}{\partial\overline{w}}-w'\frac{\partial\psi}{\partial z}+w'\overline{w}'\frac{\partial\psi}{\partial\overline{w}}-w'^{2}\frac{\partial\psi}{\partial w}\right),\\
&=\frac{2ie}{mv}\left(1+w'\overline{w}'\right)^{1/2}\left(\frac{\partial\psi}{\partial\overline{w}}-\frac{w'}{2}\frac{\partial\psi}{\partial z}+iw'\,\mathrm{Im}\left(\overline{w}'\frac{\partial\psi}{\partial\overline{w}}\right)\right)\\
&=\frac{2ie}{mv}\left(1+w'\overline{w}'\right)^{1/2}\left(\left(1+w'\overline{w}'\right)\frac{\partial\psi}{\partial\overline{w}}-\frac{w'}{2}\frac{d\psi}{dz}\right).
\end{aligned} \tag{70}$$

We can only solve the nonlinear path equation analytically in the simple case of a homogeneous magnetic field. In order to obtain insight in the general properties of the ray path, we aim to solve the equation iteratively by starting with the Gaussian approximation (28). Therefore, we transform the equation (70) to the rotating coordinate system by means of the relations (25), giving

$$\begin{aligned}
&u''-\chi'^{2}u+2i\chi'u'+i\chi''u=,\\
&=\frac{2ie}{mv}\left(1+u'\overline{u}'+\chi'^{2}u\overline{u}+i\chi'(u\overline{u}'-\overline{u}u')\right)^{1/2}\times\\
&\left(\frac{\partial\psi}{\partial\overline{u}}-\frac{u'+i\chi'u}{2}\left[\frac{\partial\psi}{\partial z}-i\,\mathrm{Im}\left((\overline{u}'-i\chi'\overline{u})\frac{\partial\psi}{\partial\overline{u}}\right)\right]\right).
\end{aligned} \tag{71}$$

We expand the expression on the right side of (71) in a powers series with respect to the slope and position coordinates. By moving the linear terms to the left side, we transform the equation (71) into the form

$$u''+2i\chi'u'+i\chi''u-\chi'^{2}u-i\frac{eB}{mv}(u'+i\chi'u)-i\frac{eB'}{2mv}u=P. \tag{72}$$

The perturbation function P comprises all nonlinear terms in $u, \bar{u}, u', \bar{u}'$ of the power series expansion. We write the perturbation function as a sum of polynomials P_n :

$$P = \sum_{n=2}^{\infty} P_n \,. \tag{73}$$

Each perturbation polynomial P_n consists of monomials of order n in $u, \bar{u}, u', \bar{u}'$. The coefficients of the monomials are formed by the multipole strengths $\Psi_m(z)$ and their derivatives. In most cases it suffices to consider only the perturbation terms up to the third order inclusively. After a rather lengthy calculation we eventually obtain for the perturbation polynomials P_2 and P_3 the relations

$$P_2 = H\bar{u}^2, H = i\frac{3e}{mv}\Psi_3 e^{-3i\chi}, \tag{74}$$

$$\begin{aligned} P_3 = & -u(u'\bar{u}' + u\bar{u}\chi'^2)\chi'^2 + u\bar{u}u'\chi'\chi'' \\ & -(u\bar{u}' - \bar{u}u')\left(u'\chi'^2 + \frac{u}{2}\chi'\chi''\right) + u^2\bar{u}\chi'\chi''' \\ & + i\left(u'\bar{u}' + u\bar{u}\chi'^2\right)\left(u'\chi' + \frac{u}{2}\chi''\right) - \frac{i}{2}u\bar{u}u'\chi''' \\ & + iu^2\bar{u}\left(\chi'^2\chi'' - \frac{1}{8}\chi^{[4]}\right) - iu(u\bar{u}' - \bar{u}u')\chi'^3. \end{aligned} \tag{75}$$

The second-order term $P_2 = H\bar{u}^2$ of the perturbation function is produced by the magnetic field of the hexapole elements, whereas the rather involved third-order term P_3 results entirely from the magnetic field of the rotationally symmetric lenses.

By substituting the expression (27) for χ' in (72), we obtain the equation

$$u'' + \chi'^2 u = P = P_2 + P_3 + ... \tag{76}$$

In order to derive a proper iteration procedure we transform this nonlinear differential equation into an integral equation. We perform the transformation by assuming that the linearly independent fundamental solutions u_α and u_π of the homogeneous equation (28) and the perturbation P are known functions of the z-coordinate. In this case, we can formally consider equation (76) as an inhomogeneous second-order linear differential equation whose homogeneous solution is given by (33). We obtain the inhomogeneous solution by employing the method of variation of coefficients. This procedure supposes that the inhomogeneous solution can be written in the form

$$u_{in} = C_\alpha(z)u_\alpha + C_\pi(z)u_\pi \,. \tag{77}$$

This solution must satisfy the path equation (76). Because the coefficients $C_\alpha(z)$ and $C_\pi(z)$ are complex functions, we can impose another requirement on these coefficients apart from (76). We obtain the information on the most appropriate condition from the derivative

$$u'_{in} = C'_\alpha u_\alpha + C'_\pi u_\pi + C_\alpha u'_\alpha + C_\pi u'_\pi \;. \tag{78}$$

In order that second-order derivatives of the coefficients do not show up in the expression for u''_{in}, we require that

$$C'_\alpha u_\alpha + C'_\pi u_\pi = 0 \,. \tag{79}$$

As a result, we obtain

$$u''_{in} = C'_\alpha u'_\alpha + C'_\pi u'_\pi + C_\alpha u''_\alpha + C_\pi u''_\pi \,. \tag{80}$$

By substituting this relation for u'' and (77) for u in equation (76) and by considering that u_α and u_π satisfy the homogeneous equation (28), we readily obtain

$$u''_{in} + \chi'^2 u_{in} = C'_\alpha u'_\alpha + C'_\pi u'_\pi = P. \tag{81}$$

The second relation in (81) together with (79) represent two linear equations for the derivatives C'_α and C'_π of the unknown coefficients C_α and C_π. By considering the Helmholtz-Lagrange relation $u_\pi u'_\alpha - u_\alpha u'_\pi = 1$, the solutions adopt the simple form

$$C'_\alpha = P u_\pi, \qquad C'_\pi = -P u_\alpha. \tag{82}$$

Integration gives

$$C_\alpha = \int_{z_o}^{z} P u_\pi dz, \qquad C_\pi = -\int_{z_o}^{z} P u_\alpha dz \,. \tag{83}$$

Note that the coefficients C_α and C_π are complex because the perturbation P is complex function. We have chosen the lower integration limit $z = z_o$ in such a way that the true ray coincides with its paraxial approximation $u_{\text{hom}} = u^{(1)} = u_o u_\pi + u'_o u_\alpha$ at the object plane z_o. The upper index (1) indicates the order the approximation of the first term of the expansion of the true ray in a series of polynomials of order n in the ray parameters $u_o, \overline{u}_o, u'_o, \overline{u}'_o$:

$$u = u(u_o, \bar{u}_o, u'_o, \bar{u}'_o; z) = \sum_{n=1}^{\infty} u^{(n)}(z). \tag{84}$$

The polynomials $u^{(n)}(z)$ with $n \geq 2$ represent the deviations of order *n* of the true ray from its ideal paraxial approximation $u^{(1)}(z)$. The coefficients of each constituent monomial of the polynomials $u^{(n)}$ are functions of the *z*-coordinate. We derive the path deviations of order *n* by means of successive iteration of the integral equation

$$\begin{aligned} u &= u^{(1)}(z) + u_\alpha \int_{z_o}^{z} P u_\pi dz - u_\pi \int_{z_o}^{z} P u_\alpha dz, \\ P &= P(u, \bar{u}, u', \bar{u}'; z). \end{aligned} \tag{85}$$

The Gaussian ray represents the initial approximation $u_1 = u^{(1)}(z)$ derived by putting $P = 0$. Each approximation u_{n+1} obtained in the n^{th} iteration step yields contributions to deviations of different order. However, we need only a finite number of iteration steps for obtaining the deviations $u^{(n)}(z)$ of a given order. The number of required steps is the smaller the lower the order of the deviation is. Because the ray parameters u_o and u'_o are small in the electron microscope, a few iterations suffice for obtaining a sufficiently accurate approximation of the true ray. The path deviation $u^{(n)}(z_i)$ at the Gaussian image plane $z = z_i$ defines the aberration of order *n*.

The so-called *primary* aberrations $\Delta u_2(z_i) = u_2(z_i) - u^{(1)}(z_i)$ are obtained in the first step of the iteration by substituting the Gaussian approximation $u_1 = u^{(1)}(z)$ for the true ray $u(z)$ in the perturbation function *P*, giving

$$\Delta u_2(z_i) = -u_\pi(z_i) \int_{z_o}^{z_i} P(u_1) u_\alpha dz = -M \int_{z_o}^{z_i} P(u_1) u_\alpha dz\,, \tag{86}$$

$$P(u_1) = P(u^{(1)}, \bar{u}^{(1)}, u'^{(1)}, \bar{u}'^{(1)}; z)\,. \tag{87}$$

In the case of magnetic round lenses, the primary aberrations comprise completely the third-order geometrical aberrations $u^{(3)}(z_i)$ and the first-order chromatic aberration which results from the chromatic perturbation function

$$P_c = -\Delta\Phi \frac{\partial T}{\partial \Phi} u = \frac{\Delta\Phi}{\Phi} \frac{eB^2}{8m\Phi} u\,. \tag{88}$$

By substituting this expression for *P* and $u^{(1)} = u'_o u_\alpha = \omega u_\alpha$ for *u* in the aberration integral (87), we obtain the axial chromatic aberration of magnetic electron lenses

$$\Delta u_c(z_i) = -M\frac{\Delta\Phi}{\Phi}C_c\omega\,,\quad C_c = \int_{z_o}^{z_i}\frac{eB^2}{8m\Phi}u_\alpha^2 dz > 0\,. \tag{89}$$

The coefficient C_c can never change sign because the integrand of its integral representation (89) is positive definite. Hence, the axial chromatic aberration of magnetic round lenses is unavoidable (Scherzer theorem).

3.1 Hexapole corrector

The hexapole corrector enables the correction of the third-order spherical aberration of round lenses. A single hexapole element introduces in first approximation a threefold deformation of the axial electron beam ($u_o = 0$). The resulting deviation of the axial rays from their ideal paraxial course $u^{(1)} = \omega u_\alpha$ produces the second-order axial astigmatism at the Gaussian imaged plane:

$$\begin{aligned} u^{(2)}(z_i) &= -u_\pi(z_i)\int_{z_o}^{z_i} P_2(u^{(1)})u_\alpha dz = -MA_2\overline{\omega}^2, \\ A_2 &= \int_{z_o}^{z_i} Hu_\alpha^3 dz. \end{aligned} \tag{90}$$

This aberration forms a threefold figure in front and behind the Gaussian image plane where it degenerates to a circle. The imaginary part of the complex coefficient A_2 determines the azimuthal orientation of the threefold aberration figure.

Apart from the second-order deviation, the hexapole field also produces a third-order deviation obtained by the second step of the iteration procedure. Because the third-order deviation is rotationally symmetric, it may be utilized to compensate for that of the round lenses provided that the second order deviation can be nullified by another hexapole element (sextupole). This compensation is indeed possible for a system consisting of two identical sextuples and a telescopic round-lens doublet, as depicted in Fig. 10. In order to find the optimum arrangement of the elements within the corrected system, we choose u_α and u_γ as the fundamental paraxial rays. Choosing u_γ instead of u_π allows us to consider the slope of u_γ as a free parameter. The first sextupole centered at the front focal plane $z_{\bar{F}1}$ of the first round lens is imaged with negative unit magnification onto the second sextupole centered at the back focal plane z_{F2} of the second round lens. In this case, the second-order path deviation $u^{(2)}$ introduced by the first sextupolepole is eliminated entirely by the second sextupole. Because the force of the hexapole field is proportional to $\overline{u}^2$, it does not affect the course of the fundamental paraxial rays u_α and u_γ. They form straight lines in front and on the far side of the round-lens doublet. We

assume that the corrector is placed behind the objective lens with focal length f_o. In this case the fundamental rays in front of the first sextupole are given by

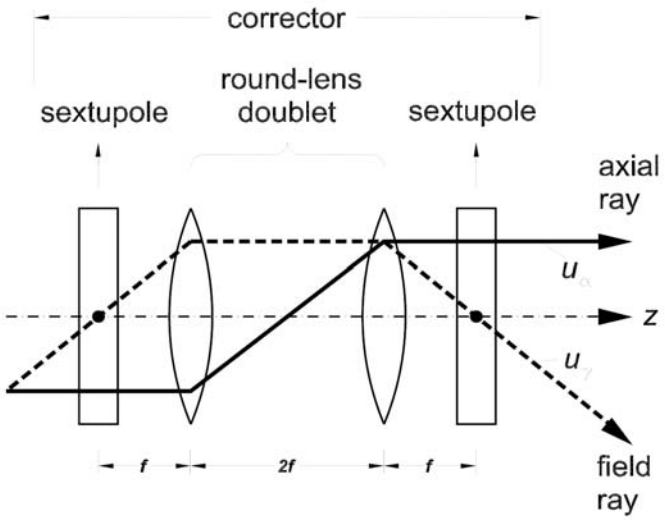

Fig. 10: Schematic arrangement of the elements of the hexapole corrector compensating for the third-order spherical aberration of round lenses.

$$u_\alpha = -f_o, \qquad u_\gamma = \frac{z - z_{\bar{F}1}}{f_o}. \tag{91}$$

The arrangement of the elements of the corrector and the path of the field ray u_γ are symmetric with respect to the mid-plane if the corrector, whereas the axial ray u_α is anti-symmetric to this plane. Hence, the fundamental rays on the far side of the round-lens doublet are

$$u_\alpha = f_o, \qquad u_\gamma = \frac{z_{F2} - z}{f_o}. \tag{92}$$

By substituting $P_2 = H\bar{u}^2$ for P in the integral equation (85), we obtain in the first step of the iteration the second-order approximation of the trajectory

$$\begin{aligned} u_2 &= u^{(1)}(z) + u^{(2)}(z), \\ u^{(2)}(z) &= u_\alpha \int_{z_o}^{z} P_{21} u_\gamma dz - u_\gamma \int_{z_o}^{z} P_{21} u_\alpha dz, \\ P_{21} &= H\left(\bar{u}_o^2 u_\gamma^2 + 2\bar{u}_o \bar{u}_o' u_\gamma u_\alpha + \bar{u}_o'^2 u_\alpha^2\right). \end{aligned} \tag{93}$$

We rewrite the second-order path deviation $u^{(2)}(z)$ in the general form

$$
\begin{aligned}
u^{(2)} &= \bar{u}_o^2 u_{\gamma\gamma}(z) + \bar{u}_o' \bar{u}_o u_{\alpha\gamma} + \bar{u}_o'^2 u_{\alpha\alpha}, \\
u_{\gamma\gamma} &= u_\alpha \int_{z_o}^{z} H u_\gamma^3 dz - u_\gamma \int_{z_o}^{z} H u_\gamma^2 u_\alpha dz, \\
u_{\alpha\gamma} &= 2u_\alpha \int_{z_o}^{z} H u_\gamma^2 u_\alpha dz - 2u_\gamma \int_{z_o}^{z} H u_\alpha^2 u_\gamma dz, \\
u_{\alpha\alpha} &= u_\alpha \int_{z_o}^{z} H u_\alpha^2 u_\gamma dz - u_\gamma \int_{z_o}^{z} H u_\alpha^3 dz.
\end{aligned}
\tag{94}
$$

The secondary fundamental rays $u_{\alpha\alpha}, u_{\alpha\gamma}$ and $u_{\gamma\gamma}$ are complex if the modified hexapole strength *H* is complex. The integral expressions (94) reveal that the secondary fundamental rays vanish on the far side of the corrector if

$$
\int_{-\infty}^{\infty} H u_\alpha^{3-\mu} u_\gamma^\mu dz = 0, \quad \mu = 0,1,2,3. \tag{95}
$$

The four conditions are satisfied by the symmetric system shown in Fig. 10 if the direction of the current within the first lens of the round-lens doublet is opposite to that of the second lens. This requirement is necessary in order that $H = i(3e/mv)\Psi_3 e^{-3i\chi}$ is symmetric with respect to the mid-plane because then the rotation angle χ_1 introduced by the first lens of the round-lens doublet is compensated for by the opposite rotation angle $\chi_2 = -\chi_1$ of the second lens. In this case, two integrands of the four integrals (95) are anti-symmetric with respect to the mid-plane of the corrector, whereas the other two are anti-symmetric with respect to the mid-planes $z_{\bar{F}1}$ and z_{F2} of the sextupoles. As a result all integrals cancel out at the far side of the corrector. Hence the second-order fundamental rays (94) vanish also in this region, as illustrated in Fig. 11.

We derive the third-order deviations introduced by the hexapole fields in the second iteration step by substituting the second-order approximation (93) for *u* in $P_2 = H\bar{u}^2$, giving

$$
\begin{aligned}
&P_2(u_2) = H\bar{u}_2^2 = H\left(\bar{u}^{(1)} + \bar{u}^{(2)}\right)^2 \\
&= H\left(\bar{u}^{(1)2} + 2\bar{u}^{(1)}\bar{u}^{(2)} + \bar{u}^{(2)2}\right) = P_2^{(2)} + P_2^{(3)} + ..., \\
&P_2^{(3)} = 2H\bar{u}^{(1)}\bar{u}^{(2)}.
\end{aligned}
\tag{96}
$$

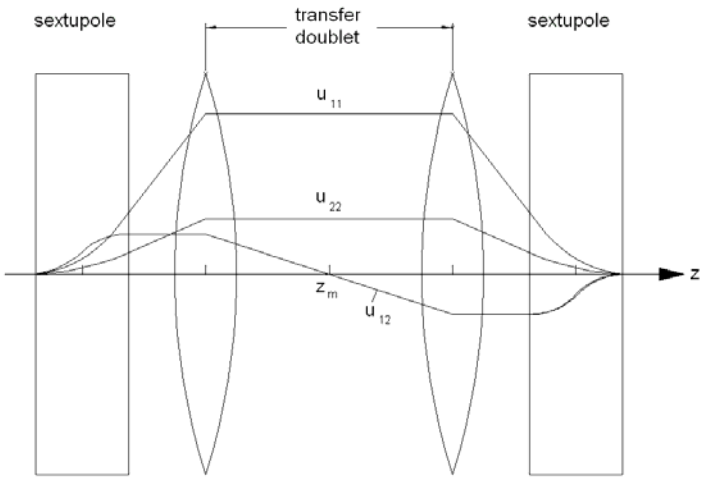

Fig. 11: Course of the secondary fundamental rays $u_{11} = u_{\alpha\alpha}, u_{12} = u_{\alpha\gamma}$ and $u_{22} = u_{\gamma\gamma}$ within the hexapole corrector.

To illustrate the iteration procedure we restrict the following calculations to axial rays which originate from the center $u_o = 0$ of the object plane. In this case the third order perturbation function (96) adopts the form

$$P_2^{(3)} = 2\omega^2 \overline{\omega} H u_\alpha \overline{u}_{\alpha\alpha} . \tag{97}$$

This expression is spherically symmetric with respect to the angle ω. By substituting $P_2^{(3)}$ for P in (86) and by considering that $u_\alpha(z_i) = 0$ at the Gaussian image plane z_i, we obtain the third-order axial (spherical) aberration of the hexapoles as

$$u_{sh}^{(3)}(z_i) = u_{\gamma i} \omega^2 \overline{\omega} C_{3h} . \tag{98}$$

$$C_{3h} = -2\int_{z_o}^{z_i} H u_\alpha^2 \overline{u}_{\alpha\alpha} dz = -2\int_{z_o}^{z_i} H u_\alpha^2 \left(u_\alpha \int_{z_o}^{z} \overline{H} u_\alpha^2 u_\gamma dz - u_\gamma \int_{z_i}^{z} \overline{H} u_\alpha^3 dz \right) dz . \tag{99}$$

The representation (98) shows that the third-order axial aberration of hexapole fields has the same form as that of round lenses

$$u_{sr}^{(3)}(z_i) = u_{\gamma i} \omega^2 \overline{\omega} C_{3r} , \quad C_{3r} > 0 . \tag{100}$$

In order to be consistent, we have defined the sign of the coefficient C_{3h} such that the aberrations (98) and (100) have the same standard form. If the integrals (99) are negative for the system shown in Fig. 10, this system can serve as a corrector compensating for the spherical aberration of round lenses because the system does not introduce any second-

order aberrations. To prove this conjecture, we approximate the field of each of the two sextupoles by box functions with axial extension *l*. Because the secondary fundamental ray $u_{\alpha\alpha}$ is symmetric with respect to the mid-plane of the corrector it suffices to calculate the contribution of the first hexapole. To simplify the calculations, we place the origin of the coordinate system at the front focal of the first transfer lens so that $z_{\bar{F}1} = 0$. By inserting the relations (91) for the primary fundamental rays into the integral expression for $u_{\alpha\alpha}$ in (94), we can perform the integrations analytically. As a result we obtauin within the interior region $-l/2 \le z \le l/2$ of the sextupole the approximation

$$u_{\alpha\alpha} = Hf_o^2\left(-\int_{-l/2}^{z} z dz + z\int_{-l/2}^{z} dz\right) = \frac{1}{2}Hf_o^2\left(z+\frac{l}{2}\right)^2. \tag{101}$$

By substituting this expression for $u_{\alpha\alpha}$ and f_o for u_α in (99), we obtain

$$C_{3h} = -4\int_{-l/2}^{l/2} Hu_\alpha^2\overline{u}_{\alpha\alpha}dz = -2H\overline{H}f_o^4\int_{-l/2}^{l/2}\left(z+\frac{l}{2}\right)^2 dz = -\frac{2}{3}|H|^2 f_o^4 l^3 < 0. \tag{102}$$

The result shows that the coefficient of the third-order spherical aberration of hexapoles has a negative sign. Its absolute value can be adjusted appropriately because the modified hexapole strength $|H|$ can be chosen arbitrarily at least in principle. Therefore, the system shown in Fig. 10 acts as third-order diverging glasses which do not affect the paraxial rays, as illustrated convincingly in Fig. 12. The spherical aberration of the round lenses and that of the corrector add up to the total spherical aberration given by

$$u_s^{(3)}(z_i) = u_{sr}^{(3)}(z_i) + u_{sr}^{(3)}(z_i) = u_{\gamma i}\omega^2\overline{\omega}C_3, \tag{103}$$

$$C_3 = C_{3r} + C_{3s} = C_{3r} - \frac{2}{3}|H|^2 f_o^4 l^3. \tag{104}$$

The relation (104) demonstrates that we achieve correction of spherical aberration by choosing

$$|H| = \frac{1}{f_o^2 l}\sqrt{\frac{3C_{3r}}{2l}}. \tag{105}$$

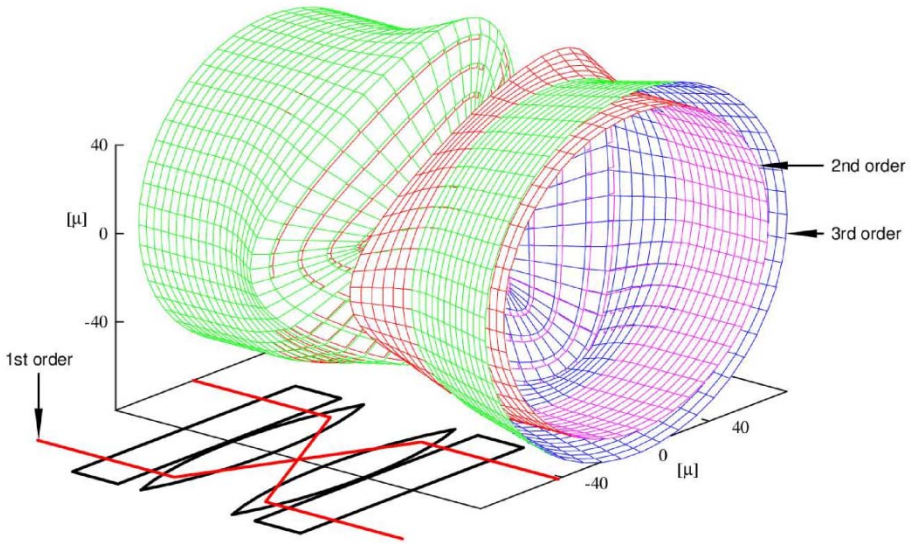

Fig. 12: Path $u = \omega u_\alpha + \overline{\omega}^2 u_{\alpha\alpha} + \omega^2 \overline{\omega} u_{\alpha\alpha\alpha}$ of the rays within the hexapole corrector, the incident rays $u_{\text{in}} = \omega u_\alpha$ run parallel to the optic axis on the mantle of a cylinder. The emerging rays form a cone whose cone angle is proportional to the third power of the starting angle $|\omega| = |\alpha + i\beta| = \sqrt{\alpha^2 + \beta^2}$ of the rays at the object plane.

3.3 Electron optical aplanat

Correction of spherical aberration does not suffice to image all points of the objects with the same resolution because the off-axial coma limits the size of the object field. In order that all points of a sufficiently extended object area are imaged with the same resolution, the off-axial third-order coma must be eliminated as well. Each imaging element has a so-called coma-free point which implies that the element does not introduce coma if the central ray $u = u_o u_\gamma$ of any off-axial bundle of rays intersects the optic axis at this point. Because we can choose the zero of the field ray u_γ arbitrarily, we place it at the coma-free point of the objective lens.

The coma-free point of the round lens is located within its field region and that of the corrector at the center of the first sextupole. Hence in order to obtain an aplanat the field ray u_γ must intersect both points. Unfortunately, we cannot match directly these points because the pole pieces of the sextupoles must be spatially separated from those of the objective lens. However, we can satisfy the requirement by optical means if we consider that the coma-free point of the telescopic round-lens doublet is given by the front focal point of its first lens. By incorporating another round lens doublet, we can image the coma-free plane of the objective lens into the coma-free plane of the corrector without introducing any coma. We realize the coma-free imaging by placing the front focal plane of the first lens of the doublet at the coma-free plane of the objective lens and the back focal plane of the second lens at the mid-lane of the first sextupole, as shown in Fig, 13. The correctors of all commercial transmission electron microscopes (TEM) realized by the CEOS company are based on this design.

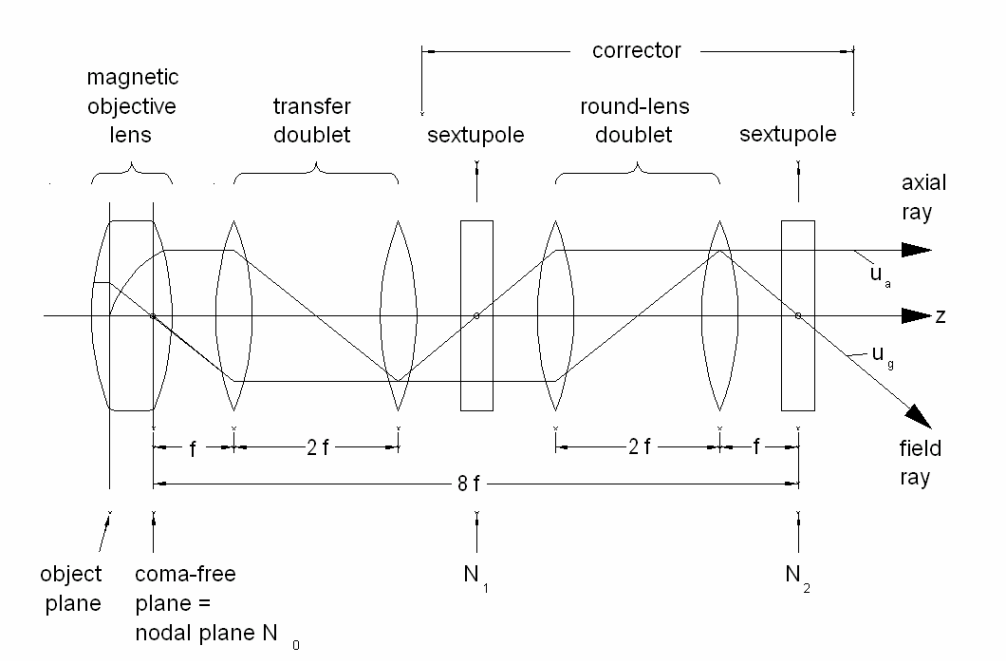

Fig. 13: Schematic arrangement of the elements of the electron-optical aplanat and path of the fundamental paraxial rays

The correction of both spherical aberration and off-axial coma allows one to tilt the direction of illumination without introducing axial coma. This possibility facilitates significantly the alignment of crystalline objects in the electron microscope because we can adjust the precise orientation of the lattice planes with respect to the direction of incidence of the plane-wave illumination by tilting the beam rather than by tilting the object. Moreover, we can align the direction of incidence by dipole fields with a much higher accuracy as the tilt angle of the specimen stage by mechanical means.